Korean J. Chem. Eng., **29**(6), 707-715 (2012)
DOI: 10.1007/s11814-011-0244-9

Numerical simulation of CO_2 absorption into aqueous methyldiethanolamine solutions

Hanna Kierzkowska-Pawlak† and Andrzej Chacuk

Faculty of Process and Environmental Engineering, Technical University of Lodz, ul. Wólczańska 213, 90-924 Łódź, Poland
(*Received 18 April 2011 • accepted 15 September 2011*)

Abstract–The CO_2 absorption rate into aqueous N-methyldiethanolamine solutions was measured using a stirred cell with a flat gas-liquid interface. The measurements were performed in the temperature range of 293.15 to 333.15 K for various amine concentrations and CO_2 partial pressures. A numerical model of mass-transfer with complex chemical reactions based on the film theory was developed to interpret the experimental results. The model predictions have been found to be in good agreement with the experimental values of CO_2 absorption rates. A comparison is made between the enhancement factor predicted from the detailed model and the approximate solution of mass transfer equations with chemical reaction. The numerical results indicate that under the present experimental conditions, the effect of the reaction between CO_2 and OH^- on the observed mass transfer rates is negligible. The detailed mass transfer model was used for simulating the CO_2 absorption process in terms of the enhancement factor under a variety of operating conditions.

Key words: CO_2 Absorption, Methyldiethanolamine, Stirred Cell, Modeling, Enhancement Factor

INTRODUCTION

Absorption of CO_2 in aqueous amine solutions has been extensively studied in the last decade. It is a process of considerable industrial importance, for example in removal of acidic compounds such as carbon dioxide and hydrogen sulfide from gas streams in the natural gas and refinery industries [1]. This technology is also currently considered as a promising method for CO_2 separation from flue gases at fossil-fuel power plants [2,3]. Among the most widely used amines, including monoethanolamine (MEA), diglycolamine (DGA), diethanolamine (DEA), diisopropanolamine (DIPA), methyldiethanolamine (MDEA) and triethanolamine (TEA), MDEA has become much more important because of its relatively high capacity, small enthalpy of reaction with acid gases and a low vapor pressure. MDEA is much less corrosive than other amines. Since the CO_2 reaction rate with a tertiary MDEA is slower than with primary or secondary ones, the addition of small amounts of fast reacting amines is necessary to apply this process in the flue gas treatment.

Many studies have been performed on the kinetics of the CO_2 reaction with aqueous MDEA [4-16]. Vaidya and Kenig provide a comprehensive overview on that subject [13]. There is agreement on the reaction mechanism which implies that tertiary amines do not react directly with CO_2. In an aqueous solution, MDEA catalyzes the CO_2 hydration reaction according to the mechanism proposed by Donaldson and Nguyen [14]. However, there are widely varying opinions in the literature on the interpretation of the kinetic data and contribution of OH^-/CO_2 reaction on the estimation of the forward rate of the MDEA-catalyzed reaction. This causes the relatively high difference in the forward rate coefficient of the MDEA-catalyzed reaction, which is ranging from 1.44 m^3 $kmol$ s^{-1} [4] to 5.15 m^3 $kmol$ s^{-1} [16] at 293 K. These discrepancies may be attributed to the different experimental techniques used and the inconsistency of the physical data such as CO_2 solubility and diffusivity applied for interpretation of the absorption rate data. Moreover, there are quantitatively inconsistent opinions on the effect of the reaction of hydroxide with CO_2 on the measured rate of CO_2 absorption into aqueous MDEA solutions [15,16].

The mathematical models of the absorption of CO_2 into MDEA aqueous solutions have been reported by a few authors [15-18]. The model of Glasscock and Rochelle [15] accounts for the multiple reactions taking place, as well as the diffusion of the ionic species involved. Concerning the mass transfer models, the film theory, Higbie-penetration theory and Danckwert's surface renewal theory have all been used for calculation of the enhancement factors. The molar fluxes of reagents were calculated from the Fick's equations. Rinker et al. [16] determined the significant reactions involved in the absorption of CO_2 into MDEA aqueous solutions as well as the effect of including or neglecting the CO_2-OH^- reaction on the forward rate coefficient of the catalyzed hydrolysis of MDEA. In this model the molar fluxes of reagents were calculated from Fick's equations. Cadours and Bouallou [17] and Kabouche et al. [18] presented more general mathematical models to describe the mass transfer with chemical reactions, which were validated for the case of the CO_2 absorption into MDEA solutions. The electrostatic potential gradient terms, with unequal diffusion coefficient for the ionic reagents, have been included in the mass transfer with complex reactions equations. In the model of Cadours and Bouallou [17], the molar fluxes of reagents were calculated from Fick's equations, while in the model of Kabouche et al. [18], the Maxwell-Stefan equations were used.

In the present work, additional data on the kinetics of the reaction between CO_2 and aqueous MDEA solutions are reported. The CO_2 absorption rate was measured using a stirred cell with a flat gas-liquid interface. The measurements were performed in the temperature range of 293.15 to 333.15 K and amine concentration range of 10 to 30% mass MDEA. A mathematical mass transfer model

†To whom correspondence should be addressed.
E-mail: kierzkow@p.lodz.pl

based on the film theory that includes all chemical reactions in CO_2-MDEA-H_2O system was developed. The model was used to predict the CO_2 absorption rate into MDEA solution and the corresponding mass transfer enhancement factor. The experimental absorption rate data are compared with the data predicted by the mathematical mass transfer model. The applicability of an approximate method of solution for absorption with chemical reaction is also discussed. The approximate model takes into account only the main reaction between CO_2 and MDEA and treats it as irreversible and pseudo-first order. Based on the computational results, the comparison between the detailed mathematical model and the simplified one is demonstrated. The detailed mass transfer model was used for simulating the CO_2 absorption process in terms of the enhancement factor for a variety of operating conditions.

DESCRIPTION OF CO_2 ABSORPTION INTO AQUEOUS SOLUTIONS OF MDEA

1. A Detailed Model

1-1. Reaction Scheme

The following reactions may take place when CO_2 is absorbed into an aqueous solution of MDEA [10]:

$$CO_2 + H_2O + MDEA \xleftrightarrow{K_1, k_1} MDEAH^+ + HCO_3^- \quad (1)$$

$$CO_2 + OH^- \xleftrightarrow{K_2, k_2} HCO_3^- \quad (2)$$

$$HCO_3^- + OH^- \xleftrightarrow{K_3} CO_3^{2-} + H_2O \quad (3)$$

$$MDEAH^+ + OH^- \xleftrightarrow{K_4} MDEA + H_2O \quad (4)$$

According to the literature, reactions (1) and (2) have finite rates, whereas the reactions (3) and (4) are instantaneous as they involve only a proton transfer.

For convenience, the chemical species in reactions (1)-(4) are renamed as follows:

$A \equiv CO_2$, $B \equiv MDEA$, $C \equiv MDEAH^+$, $D \equiv HCO_3^-$, $E \equiv OH^-$, $F \equiv CO_3^{-2}$

1-2. Liquid Bulk Concentrations

To calculate the rate of CO_2 absorption it is necessary to know the equilibrium concentrations of the reactants in the bulk of the liquid phase. These concentrations C_{iL}^{δ}, i=A, …, F of individual reaction species were determined from the overall concentration of MDEA and the initial CO_2 loading according to the following:

Overall MDEA balance:

$$C_{BL}^{\delta} + C_{CL}^{\delta} = C_{BL}^{ov} \quad (5)$$

Electroneutrality balance:

$$C_{CL}^{\delta} - C_{DL}^{\delta} - C_{EL}^{\delta} - 2C_{FL}^{\delta} = 0 \quad (6)$$

Overall carbon balance:

$$C_{AL}^{\delta} + C_{FL}^{\delta} + C_{DL}^{\delta} = \alpha \cdot C_{BL}^{ov} \quad (7)$$

Equilibrium equations:

$$K_2 = \frac{C_{DL}^{\delta}}{C_{AL}^{\delta} C_{EL}^{\delta}} \quad (8)$$

$$K_3 = \frac{C_{FL}^{\delta}}{C_{DL}^{\delta} C_{EL}^{\delta}} \quad (9)$$

$$K_4 = \frac{C_{BL}^{\delta}}{C_{CL}^{\delta} C_{EL}^{\delta}} \quad (10)$$

Eqs. (5)-(10) form a system of six nonlinear algebraic equations with six unknowns C_{iL}^{δ}, i=A, …, F. In this paper the system of these equations was solved using Marquardt's iterative method [19,20].

1-3. Reaction Kinetics

Reactions (1) and (2) are reversible reactions that occur with a finite rate. Their overall rates are given by the following reaction rate expressions:

$$r_1 = k_1 C_{AL} C_{BL} - \frac{k_1}{K_1} C_{CL} C_{DL} \quad (11)$$

$$r_2 = k_1 C_{AL} C_{EL} - \frac{k_2}{K_2} C_{DL} \quad (12)$$

Reactions (3) and (4) are reversible reactions but occur with infinite rate, so their overall rates are equal to zero; therefore,

$$K_3 = \frac{C_{FL}}{C_{DL} C_{EL}} \quad (13)$$

$$K_4 = \frac{C_{BL}}{C_{CL} C_{EL}} \quad (14)$$

1-4. Mathematical Description

Mathematical description of the CO_2 absorption into an aqueous solution of MDEA in the reactor under consideration was formulated by adopting the following simplifying assumptions:

- the process is steady and isothermal,
- liquid phase is a dilute solution,
- the surface of the mass transfer is flat,
- CO_2 concentration on the gas-liquid interface results from Henry's law,
- concentrations of the chemical species in the liquid bulk are constant and correspond to the equilibrium concentrations,
- amine and ions formed by chemical reactions are non-volatile.

For the case under consideration, the mass transfer in the layer of liquid of thickness δ is described by the equations:

$$D_{iL} \frac{d^2 C_{iL}}{dx^2} = -\sum_{j=1}^{2} \nu_{ij} r_j, \quad i = A, \ldots, D \quad (17)$$

Concentrations of species E and F result from Eqs. (13) and (14):

$$C_{EL} = \frac{1}{K_4} \frac{C_{BL}}{C_{CL}} \quad (18)$$

$$C_{FL} = \frac{K_3}{K_4} \frac{C_{BL} C_{DL}}{C_{CL}} \quad (19)$$

The ordinary differential equations which describe the mass transfer with complex chemical reactions were combined in such a way so as to eliminate the very large reaction rates for two instantaneous reactions (3) and (4). Since these reactions are assumed to be at equilibrium, their equilibrium constant expressions were used to complete the set of equations which are required to solve for the concentration profiles of all chemical species in the liquid film.

Molar flux of CO_2 absorption from the interfacial surface to the liquid phase results from the equation:

$$N^*_{AL} = -D_{AL}\left(\frac{dC_{AL}}{dx}\right)_{x=0} \quad (20)$$

The boundary conditions of Eqs. (17) are as follows:

$$x = 0 \;\; C_{AL} = C^*_{AL} = \frac{p^0_A}{H}, \;\; \frac{dC_{iL}}{dx} = 0, \;\; i = B, \ldots, F \quad (21)$$

$$x = \delta_L \;\; C_{iL} = C^\delta_{iL}, \;\; i = A, \ldots, F \quad (22)$$

A mathematical model of CO_2 absorption, described by Eqs. (17)-(20) with the boundary conditions (21) and (22), is valid for the steady conditions. For the process realized in the batch reactor, the model may be used only to determine the CO_2 absorption rate in the initial moment when the assumption of constant concentrations of reactants in the liquid bulk is justified.

The enhancement factor of absorption is given by the equation:

$$E_A = \frac{N^*_{AL}}{k_{AL}(C^*_{AL} - C^\delta_{AL})} \quad (23)$$

The enhancement factor is defined as the ratio of the absorption rate of a gas in the liquid in the presence of a chemical reaction to the absorption rate in the absence of a reaction at identical concentration differences of the absorbing gas between the interface and the liquid bulk.

Eqs. (17)-(19) with boundary conditions (21) and (22) are classified as two-point boundary problem for ordinary differential equations of second order. In this work, the differential equations were converted to a dimensionless canonical form and the problem was solved as a two-point boundary problem for ordinary differential equations of the first order. The substitution of

$$s = \frac{x}{\delta}, \;\; \Phi_A = \frac{C_{AL}}{C^*_{AL}}, \;\; \Phi_i = \frac{C_{iL}}{C^\delta_{iL}}, \;\; i = B, \ldots, F \quad (24)$$

$$y_1 = \frac{d\Phi_A}{ds}, \;\; y_2 = \Phi_B, \;\; y_3 = \Phi_C, \;\; y_4 = \Phi_D,$$
$$y_5 = \Phi_A, \;\; y_6 = \frac{d\Phi_B}{ds}, \;\; y_7 = \frac{d\Phi_C}{ds}, \;\; y_8 = \frac{d\Phi_D}{ds} \quad (25)$$

leads to the dimensionless canonical form of differential Eqs. (17)-(19) as follows [21]:

$$\frac{dy_1}{ds} = Ha^2 y_2 y_5 - a_1 y_3 y_4 + a_2 y_5 y_9 - a_3 y_4$$
$$\frac{dy_2}{ds} = y_6$$
$$\frac{dy_3}{ds} = y_7$$
$$\frac{dy_4}{ds} = y_8$$
$$\frac{dy_5}{ds} = y_1$$
$$\frac{dy_6}{ds} = a_4 y_2 y_5 - a_5 y_3 y_4$$
$$\frac{dy_7}{ds} = -a_6 \frac{dy_6}{ds}$$
$$\frac{dy_8}{ds} = -a_7 \frac{dy_1}{ds}$$
$$y_9 = a_8 \frac{y_2}{y_3}$$
$$y_{10} = a_9 y_4 y_9 \quad (26)$$

where:

$$Ha^2 = \frac{k_1 C^\delta_{BL} D_{AL}}{k^2_{AL}}$$
$$a_1 = \frac{1}{K_1} \frac{C^\delta_{CL} C^\delta_{DL}}{C^*_{AL} C^\delta_{BL}} Ha^2, \;\; a_2 = \frac{k_2}{k_1} \frac{C^\delta_{EL}}{C^\delta_{BL}} Ha^2, \;\; a_3 = \frac{k_2}{k_1 K_2} \frac{C^\delta_{DL}}{C^*_{AL} C^\delta_{BL}} Ha^2$$
$$a_4 = \frac{k_{AL}}{k_{BL}} \frac{C^*_{AL}}{C^\delta_{BL}} Ha^2, \;\; a_5 = \frac{1}{K_1} \frac{k_{AL}}{k_{BL}} \frac{C^\delta_{CL} C^\delta_{DL}}{C^\delta_{BL} C^\delta_{BL}} Ha^2$$
$$a_6 = \frac{k_{BL}}{k_{CL}} \frac{C^\delta_{BL}}{C^\delta_{CL}}, \;\; a_7 = \frac{k_{AL}}{k_{DL}} \frac{C^*_{AL}}{C^\delta_{DL}}, \;\; a_8 = \frac{1}{K_4} \frac{C^\delta_{BL}}{C^\delta_{CL} C^\delta_{EL}}, \;\; a_9 = K_3 \frac{C^\delta_{DL} C^\delta_{EL}}{C^\delta_{FL}} \quad (27)$$

The boundary conditions of Eqs. (26) will take the form:

$$s = 0 \;\; y_5 = 1, \; y_i = 0, \; i = 6, 7, 8 \quad (28)$$

$$s = 1 \;\; y_i = 1, \; i = 2, 3, 4, \; y_5 = \Phi^\delta_A \quad (29)$$

The method of solution of the model Eqs. (26) with boundary conditions (28) and (29) was described in detail in the previous paper [21]. In the model, one must assume a certain CO_2 loading in the liquid bulk which is used as a boundary condition. It was checked that decreasing CO_2 loading below $\alpha < 0.005$ (mol CO_2/mol MDEA) did not influence the computed results of the mass transfer rate and enhancement factor. Thus, the computed results for $\alpha = 0.005$ (mol CO_2/mol MDEA) were used for comparison with experimental data where the solution was not initially loaded with CO_2 ($\alpha = 0$).

2. An Approximate Model

In the simplified mass transfer model we took into account only one chemical reaction (1) and treated it as irreversible. In the case where the operating conditions for the absorption were selected in a way to ensure that the chemical reaction takes place in the fast pseudo-first order regime, without depletion of the amine near the gas-liquid interface, the following conditions should hold [20]:

$$3 < Ha << E_i \quad (30)$$

where Hatta number, Ha is given by:

$$Ha = \frac{\sqrt{k_1 C^\delta_{BL} D_{AL}}}{k_{AL}} \quad (31)$$

The enhancement factor for an irreversible, instantaneous reaction E_i is defined as follows:

$$E_i = 1 + \frac{D_{BL} C^\delta_{BL}}{\nu_{B1} D_{AL} C^*_{AL}} \quad (32)$$

The general expression for CO_2 absorption rate in the case where the bulk CO_2 concentration is equal to zero has the following form:

$$N^*_{AL} = E_A k_{AL} C^*_{AL} \quad (33)$$

When condition (30) is satisfied, the enhancement factor E_A is equal to the Ha number:

$$E_A = Ha \quad (34)$$

Thus, the approximate rate of mass transfer of CO_2 becomes

$$N_{AL}^{*} = C_{AL}^{*}\sqrt{k_1 C_{BL}^{\delta} D_{AL}} \quad (35)$$

As can be seen from Eq. (35), in the pseudo-first-order chemical absorption regime, the absorption rate is independent of the liquid side mass transfer coefficient k_{AL} and hence it should not depend on the stirring speed.

3. Model Parameters

To use the detailed mathematical model and the simplified one to estimate the CO_2 absorption rate, the variety of physicochemical properties of the system under consideration must be known. The values of physical mass transfer coefficient of CO_2 in aqueous MDEA solutions were obtained from a mass transfer correlation between dimensionless numbers (Sh_L, Re_L, Sc_L) that has been established for our apparatus from CO_2 absorption experiments into the pure water and N_2O absorption into aqueous MDEA solutions in the following form [21]:

$$Sh_L = 0.3929 Re_L^{0.6632} Sc_L^{0.33} \quad (36)$$

The values of relevant physicochemical properties including densities and viscosities of aqueous MDEA solutions, CO_2 solubility, and the diffusion coefficients of all chemical species in the aqueous MDEA are taken from literature [7,22,23,17] and were summarized in our previous paper [21]. The diffusion coefficients of ionic species are assumed to be equal to that of MDEA. It was checked that introducing different values of diffusion coefficients of ions, as in the model of Glasscock and Rochele [15], did not influence the predicted absorption rate. The Arrhenius law for the reaction rate constant k_1 in Eq. (11) is taken from Ko et al. [8], who studied CO_2 absorption into aqueous MDEA solutions in the temperature range 293-353 K. The reaction rate constant k_2 was calculated from the correlation presented by Pinsent et al. [25] over the temperature range 273-313 K. According to Jamal et al. [10,11], this correlation can be extrapolated to higher temperatures up to 343 K. The expressions for equilibrium constants K_1-K_4 of chemical reactions (1-4) as well as reaction rate constants k_1 and k_2 are also summarized in the previous paper [21].

EXPERIMENTAL

1. Apparatus and Procedure

The measurements were performed in the heat flow reaction calorimeter (CPA-Chemical Process Analyser, ChemiSens AB, Sweden) which is a fully automated and computer-controlled stirred reactor vessel with possibility of an on-line measurement of thermal power developed by the process. The reactor is submerged in the thermostating liquid bath. A Peltier element mounted inside the bottom of the reactor serves as an efficient heating and cooling device and keeps the temperature constant to ±0.1 K. The experimental apparatus (Fig. 1) was modified to measure acid gas absorption and desorption rates from alkanolamine solutions under unsteady state conditions and was described in detail elsewhere [21].

A series of experiments was conducted at temperature range of 293 to 333 K. The initial MDEA concentration in the aqueous solution was varied in the range of 0.83-2.7 kmol/m^3, which corresponds to amine weight fraction from 10 to 30 mass%. In each experiment, the reactor was charged with 100 cm^3 of the alkanolamine solution. After the reactor was filled with the desired solution, the liquid was

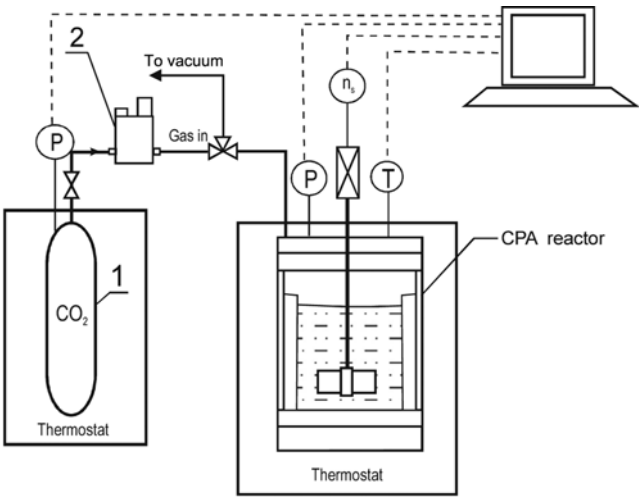

Fig. 1. Experimental set-up.
1. Storage tank
2. Downstream pressure regulator
n_s. Stirring speed transducer
T. Temperature sensors
P. Pressure transducers

degassed and heated to the set temperature under stirring conditions. When the thermal equilibrium was established, e.g., the temperature in the reactor became constant to ±0.01 K, the stirring was stopped for a moment. Pure gas from the CO_2 reservoir was then introduced during a very short time in the upper part of the cell. The resulting initial pressure in the range of 25 to 110 kPa was set by the back pressure regulator (Brooks, 5866). Then the absorption process was initiated by switching on the stirrer at the stirring speed of 150 min^{-1}. The decrease in the system pressure due to absorption of the gas was monitored by the pressure transducer, and the "p_A vs. t" data were recorded as a function of time until the gas-liquid equilibrium state was reached. The initial "p_A vs. t" data from t=0 to 60 s were plotted and the absorption rate was calculated from the value of the slope ($-dp_A/dt$). This method based on the fall-in-pressure technique was used previously by other investigators [5,12] and enabled a simple and straightforward estimation of the absorption rates.

The CO_2 partial pressure in the reactor, p_A, was calculated according to the total pressure in the system P measured by the pressure transducer, corrected for solution vapor pressure by use of Raoults's law. In these calculations, the amine vapour pressure was neglected, as it was very small as compared to the solvent vapour pressure.

The chemicals employed, CO_2 (L'Air Liquide, 99.995 vol% pure) and MDEA (Fluka, 99 mass% pure), were used without any further purification. Alkanolamine aqueous solutions were prepared from the distilled, deionized water. Experiments were performed with initial CO_2 loadings of the solutions equal to zero. The solution volume was maintained at 100±0.1 cm^3 in each experiment. The respective mass of the solutions was determined within ±0.01 g. In the range of stirring speed of 100 to 170 min^{-1}, the absorption rate was independent of the stirring speed indicating a pseudo-first order regime. Thus, in the present work all experimental runs were performed at a constant stirring speed of 150 min^{-1}. Mixing of the liquid under such a stirring speed did not affect the smoothness of the gas liquid interface, which could be easily estimated. The gas-liquid inter-

face, A, was determined as $23.5\pm0.5\cdot10^{-4}$ m^2.

2. Calculation of Experimental Absorption Rate and Enhancement Factor

The initial experimental CO_2 absorption rate can be calculated by the mass balance in the reactor gas phase according to:

$$-\frac{V_G}{R\cdot T\cdot A}\frac{dp_A}{dt}=N_{AL}^{*} \tag{37}$$

In Eq. (37), the ideal gas equation was applied. This measurement method based on the recorded pressure decrease versus time enabled a simple and straightforward estimation of the experimental absorption rate. The uncertainty in the experimental mass transfer rate has been estimated to be ±2.6%.

The CO_2 bulk concentration C_{AL}^{δ} was assumed to be zero at the initial stage of absorption, while the CO_2 concentration at the interface results from Henry's law at the initial pressure, p_A^o. The corresponding experimental enhancement factor E_A was calculated from the Eq. (23).

RESULTS AND DISCUSSION

Several CO_2 absorption experiments into MDEA aqueous solutions were carried out in the temperature range of 293 to 333 K.

Table 1. Experimental results and theoretical predictions

	Experimental						Detailed model		Approximate model		
T	C_{BL}^{ov}	p_A^o	$C_{AL}^{*}\cdot10^3$	$k_{AL}\cdot10^5$	$N_{AL}^{*}\cdot10^6$	E_A	$N_{AL}^{*}\cdot10^6$	E_A	$N_{AL}^{*}\cdot10^6$	E_A=Ha	E_i
K	kmol/m^3	kPa	kmol/m^3	m/s	kmol/m^2 s	-	kmol/m^2 s	-	kmol/m^2 s	-	-
293.15	1.706	94.13	32.3	1.58	2.16	4.23	2.38	4.65	2.52	4.92	27
293.15	1.706	94.25	32.4	1.58	2.17	4.22	2.38	4.65	2.52	4.92	27
293.15	1.706	67.41	23.2	1.58	1.62	4.41	1.73	4.72	1.80	4.92	37
293.15	1.706	59.04	20.3	1.58	1.55	4.83	1.52	4.74	1.58	4.92	42
293.15	1.706	52.30	18.0	1.58	1.38	4.84	1.35	4.76	1.40	4.92	47
293.15	1.706	46.80	16.1	1.58	1.23	4.82	1.22	4.77	1.25	4.92	52
293.15	2.586	81.81	25.9	1.02	2.01	7.60	1.95	7.37	2.03	7.68	54
293.15	2.586	65.23	20.6	1.02	1.66	7.90	1.57	7.46	1.61	7.68	68
293.15	2.586	96.09	30.4	1.02	2.04	6.60	2.26	7.30	2.38	7.68	47
293.15	2.586	77.23	24.4	1.02	2.07	8.31	1.84	7.39	1.91	7.68	58
293.15	2.586	76.82	24.3	1.02	2.46	9.92	1.83	7.40	1.90	7.68	58
293.15	2.586	54.90	17.4	1.02	1.34	7.53	1.33	7.52	1.36	7.68	81
293.15	2.586	48.96	15.5	1.02	1.25	7.90	1.19	7.56	1.21	7.68	91
293.15	2.586	34.49	10.9	1.02	1.12	10.1	0.85	7.66	0.85	7.68	128
313.15	0.839	77.06	17.4	3.80	2.66	4.02	2.69	4.07	2.62	3.96	22
313.15	0.839	58.15	13.1	3.80	2.21	4.43	2.09	4.19	1.98	3.96	29
313.15	0.839	55.64	12.6	3.80	1.93	4.03	2.01	4.21	1.89	3.96	30
313.15	0.839	43.86	9.9	3.80	1.68	4.46	1.63	4.33	1.49	3.96	38
313.15	0.839	36.41	8.2	3.80	1.39	4.45	1.38	4.42	1.24	3.96	46
313.15	1.693	87.96	8.9	2.74	3.61	6.96	3.42	6.59	3.48	6.70	43
313.15	1.693	57.77	12.4	2.74	2.19	6.43	2.32	6.81	2.29	6.70	66
313.15	1.693	37.83	8.1	2.74	1.60	7.18	1.57	7.03	1.50	6.70	100
313.15	1.693	35.88	7.7	2.74	1.66	7.84	1.50	7.06	1.42	6.70	105
313.15	1.693	34.69	7.5	2.74	1.40	6.85	1.45	7.08	1.37	6.70	109
313.15	2.560	87.33	17.9	1.90	3.53	10.39	3.31	9.73	3.42	10.04	75
313.15	2.560	59.40	12.2	1.90	2.24	9.66	2.31	9.99	2.32	10.04	109
313.15	2.560	43.69	9.0	1.90	1.93	11.35	1.74	10.22	1.71	10.04	149
333.15	0.834	66.68	10.4	5.73	3.50	5.88	3.61	6.04	3.27	5.46	36
333.15	0.834	42.71	6.7	5.73	2.11	5.53	2.50	6.53	2.09	5.46	55
333.15	0.834	33.87	5.3	5.73	1.77	5.84	2.07	6.83	1.66	5.46	70
333.15	1.681	100.06	14.9	4.33	5.68	8.80	5.74	8.93	5.80	9.01	54
333.15	1.681	63.59	9.5	4.33	3.07	7.48	3.86	9.43	3.69	9.01	84
333.15	1.681	43.70	6.5	4.33	2.49	8.81	2.78	9.87	2.53	9.01	122
333.15	1.681	26.00	3.9	4.33	1.82	10.86	1.77	10.58	1.51	9.01	204
333.15	2.53	167.1	23.8	3.17	11.5	15.24	8.99	11.69	9.85	13.07	54
333.15	2.53	100.1	14.2	3.17	5.58	12.40	5.75	12.49	5.90	13.07	90
333.15	2.53	71.9	10.2	3.17	4.26	13.19	4.27	12.93	4.24	13.07	125
333.15	2.53	46.7	6.7	3.17	3.30	15.67	2.89	13.45	2.76	13.07	192
333.15	2.53	27.9	4.0	3.17	2.05	16.28	1.80	14.07	1.65	13.08	320

All experiments were performed with initial CO_2 loadings of the solutions equal to zero as the solvent was degassed in the reactor before the run. The data on the CO_2 absorption kinetics including the measured initial absorption rates and enhancement factors obtained from Eqs. (37) and (23) are listed in Table 1. For each experiment, the theoretical mass transfer rate and the enhancement factor were calculated by the use of the proposed numerical model and reported in Table 1 for comparison. The input data for the model were the initial amine concentration, the initial pressure of absorption p_A^o and the physical mass transfer coefficient k_{AL}, which is a function of the stirring speed and relevant physicochemical properties. For the aim of identifying the chemical absorption regime, the estimates for Hatta number and the enhancement factor corresponding to the instantaneous, irreversible reaction, E_i are also reported. The values of Ha number and E_i indicate that the absorption takes place in the fast pseudo-first order reaction regime so the use of approximate method expressed by Eq. (35) for predicting the CO_2 absorption rate is justified. The relevant values of the N_{AL}^* calculated from this simplified model of absorption are also reported in Table 1.

As can be seen from the tabulated data, the numerical model gives good prediction of CO_2 absorption rate. However, with the increase of amine concentration and temperature, the model tends to underestimate the experimental mass transfer rate.

From the data at all temperatures given in Table 1, the CO_2 absorption rates predicted by the detailed model are in good agreement with the experimental results. The average deviation RMSD (Root Mean Square Deviation) between predicted and experimentally measured rates of CO_2 absorption was 1.12%. The RMSD was calculated according the following formula:

$$\mathrm{RMSD}=\frac{1}{n}\sqrt{\sum_{i=1}^{n}\left(\frac{N_{AL\,exp,i}^{*}-N_{AL\,theor,i}^{*}}{N_{AL\,exp,i}^{*}}\right)^{2}} \qquad (38)$$

The absorption rates predicted by the simplified model are also very close to those computed from the detailed numerical model and the respective estimate of RMSD is 1.18%.

Over a wide range of operating conditions studied, both models give almost the same results of predicted CO_2 absorption rates and the differences between these models are within uncertainty of the measured absorption rate. It should be stressed, however, that the simplified model is valid only for pseudo-first order regime of chemical reaction, while the proposed mathematical model is more general and can be applied in the case of complex chemical reactions irrespective of the regime of absorption.

Table 2. Simulation parameters for the CO_2-H_2O-MDEA system at 313 K

Parameter	Value	Reference
T	313.15 K	-
C_{BL}^{ov}	1.693 kmol m^{-3}	-
α	0.005 mol CO_2/mol MDEA	-
k_2	$2.456\cdot10^{4}$ m^3 $kmol^{-1}$ s^{-1}	[25]
k_1	13.005 m^3 $kmol^{-1}$ s^{-1}	[8]
K_1	106.944	[11]
K_2	$1.736\cdot10^{7}$ m^3 $kmol^{-1}$	[11]
K_3	$2.103\cdot10^{3}$ m^3 $kmol^{-1}$	[11]
K_4	$1.623\cdot10^{5}$ m^3 $kmol^{-1}$	[11]
ρ_L	1010 kg m^{-3}	[17]
η_L	$1.319\cdot10^{-3}$ Pa s	[17]
D_{AL}	$1.534\cdot10^{-9}$ m^2 s^{-1}	[22]
D_{BL}	$7.274\cdot10^{-10}$ m^2 s^{-1}	[7]
k_{AL}	$2.472\cdot10^{-5}$ m s^{-1}	[21]
H	4.646 MPa m^{-3} $kmol^{-1}$	[23]

Table 3. Results of the simulation in the bulk region for the conditions reported in Table 2

Species	Bulk concentrations (kmol m^{-3})
CO_2	$2.673\cdot10^{-7}$
MDEA	1.679
$MDEAH^+$	0.014
HCO_3^-	$3.367\ 10^{-3}$
OH^-	$7.235\ 10^{-4}$
CO_3^{2-}	$5.107\cdot10^{-3}$

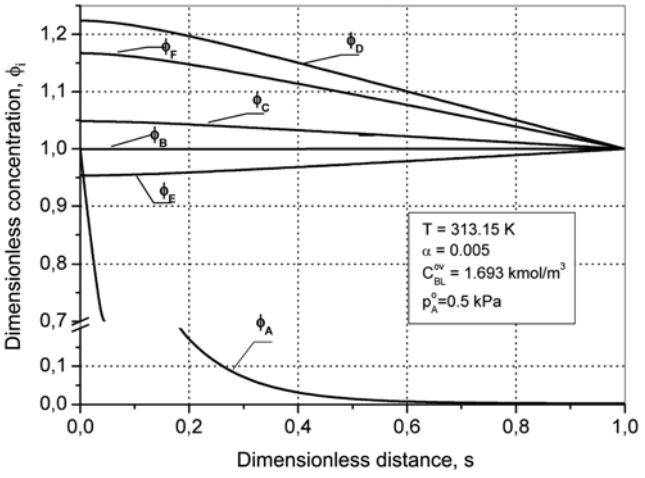

Fig. 2. Concentration profiles calculated with the detailed model at a low CO_2 partial pressure (Simulation parameters are reported in Table 2).

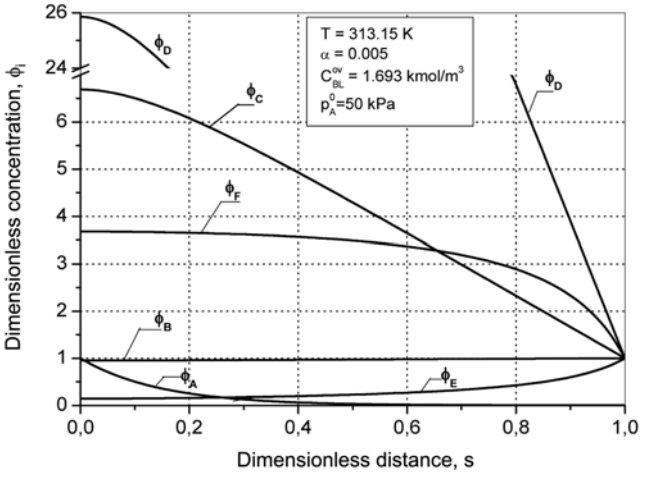

Fig. 3. Concentration profiles calculated with the detailed model at a high CO_2 partial pressure.

The simulation parameters for a certain case, which should help to verify the results computed by the detailed model, are reported in Table 2. The estimates of the species concentration in the liquid bulk are presented in Table 3. In Figs. 2 and 3, the concentration profiles of CO_2 and other species calculated by the accurate model with a low CO_2 partial pressure of 0.5 kPa and a high pressure of 50 kPa are plotted versus position in the liquid film. In Fig. 2, the profiles calculated for a low pressure show very slight depletion of the OH^- ions near the gas-liquid interface (Φ_E). In this case, the concentration of OH^- is significant and the CO_2/OH^- reaction has the largest effect on the CO_2 absorption rate. At a high CO_2 partial pressure (Fig. 3), the hydroxide becomes depleted in the liquid film, and in this case the influence of the CO_2/OH^- reaction on the overall mass transfer rate can be neglected because the MDEA has a major contribution. This observation agrees with the conclusions of Glasscock et al. [15]. However, the direct comparison of the results in terms of concentration profiles is impossible as the previous authors reported neither the bulk nor interfacial concentrations in tabulated form.

For the above conditions, the CO_2 absorption rates and the enhancement factors were predicted by the detailed model and compared to the results computed from the simplified model (Table 4). As can be seen from these data, the simplified model underestimates the CO_2 absorption rate at low pressures (p_A^o=0.5 kPa) due to neglecting the CO_2/OH^- reaction. For higher pressures (p_A^o=50 kPa), the predicted mass transfer rate from both models are the same, which supports the previous findings.

Our next step was to establish the importance of the CO_2/OH^- reaction quantitatively. This was simply accomplished by setting the reaction rate constant k_2=0 in the detailed model, which was similarly done by Glasscock and Rochelle [15]. In this case, the concentrations of all species in the liquid bulk will be the same as previously reported in Table 3. The model results after the proposed modifications are also presented in Table 4. For a low CO_2 partial pressure, the predicted absorption rate by the model after excluding the CO_2/OH^- reaction is about one-third smaller than that computed from the "full" mathematical model. For a higher pressure, both predicted values are almost the same, indicating that the CO_2/OH^- reaction can be neglected under these conditions without any loss of accuracy. To conclude, at low CO_2 concentrations, which correspond to low CO_2 partial pressures, there is no depletion of MDEA and hydroxide in the liquid film, and both chemical reactions, CO_2/MDEA and CO_2/OH^-, take place in the pseudo-first order regime (there are very small gradients in hydroxide - Φ_E and MDEA - Φ_B) and thus the reaction with hydroxide should be also incorporated in the approximate model. For these conditions, the product of k_1 and amine concentration of 21.8 s^{-1} is obtained. Using the bulk concentration of OH^-, the product of k_2 and hydroxide concentration of 17.8 s^{-1} is calculated, which is almost as high as the prior one and cannot be neglected.

From the simulations we concluded that in the present absorption experiments, the OH^- depletion near the gas-liquid interface was small and the OH^- contribution to the observed absorption rate was negligible.

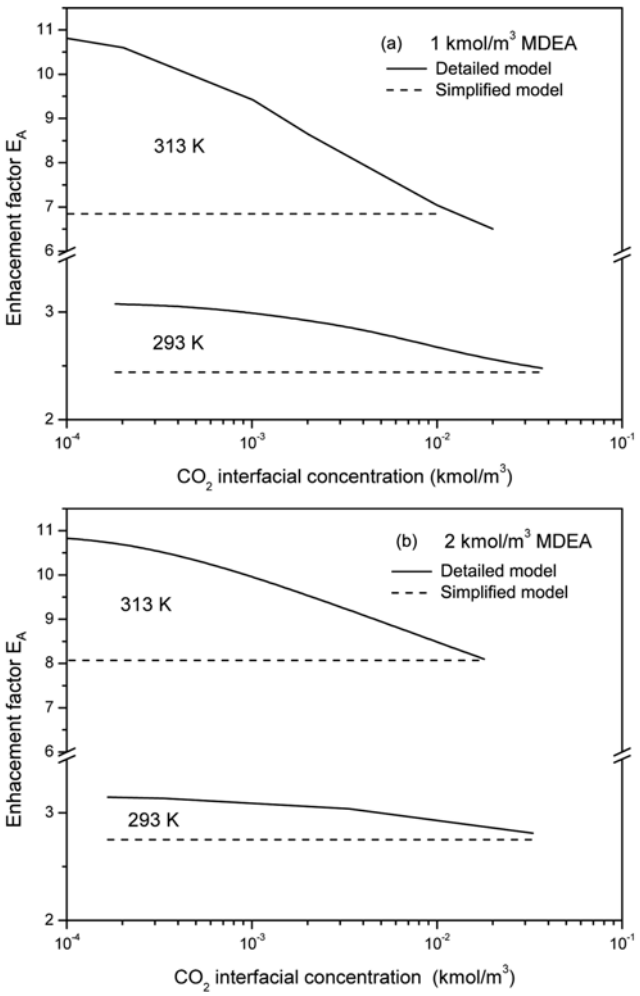

Fig. 4. Effect of CO_2 interfacial concentration on the enhancement factor for (a) -1 and (b) -2 kmol/m^3 MDEA solution. Comparison with the approximate solution for the pseudo-first-order irreversible reaction (k_{AL}=2.8·10^{-5} m/s, α=0.005).

Table 4. Predicted absorption rates and enhancement factors from the detailed and the simplified model for the CO_2 absorption into MDEA solutions for different CO_2 partial pressures

	The detailed model	The simplified model	The detailed model with setting k_2=0
Variable		p_A^o=0.5 kPa	
N_{AL}^* [kmol m^{-2} s^{-1}]	2.62·10^{-8}	1.98·10^{-8}	1.962·10^{-8}
E_A	8.89	6.7	6.67
		p_A^o=50 kPa	
N_{AL}^* [kmol m^{-2} s^{-1}]	2.031·10^{-6}	2.031·10^{-6}	1.912·10^{-6}
E_A	6.88	6.7	6.48

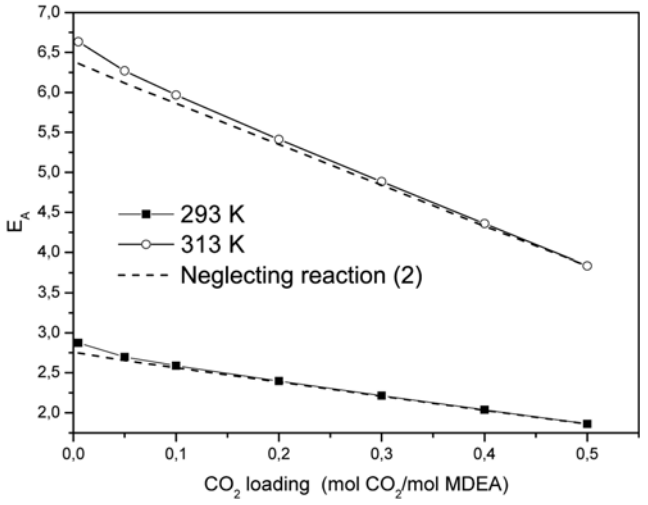

Fig. 5. Predicted enhancement factor for the absorption of CO_2 into 2 kmol/m^3 solution of MDEA as a function of CO_2 loading. The dashed line was generated from the detailed model by neglecting the reaction (2) (k_{AL}=2.8·10^{-5} m/s, C^*_{AL}=0.017 kmol/m^3).

The simulation results of the enhancement factors predicted by the detailed and simplified model at different temperatures and amine concentrations as a function of CO_2 interfacial concentration are shown in Fig. 4. The shape of the enhancement curves is similar to earlier observations [15,17]. The differences between the numerical and approximate solution of mass transfer with a single, irreversible chemical reaction under the conditions where 3<Ha<<E_i is fulfilled, increase with decreasing MDEA concentration and CO_2 partial pressure. These differences increase with temperature. At a fixed temperature, the CO_2 partial pressure and MDEA concentration, the enhancement factor computed with the presented model increases with the decrease of k_{AL}, while the corresponding approximate E_A remains constant as expected from Eq. (34). For example, for the following conditions-313 K, 1 kmol/m^3 MDEA, C^*_{AL}= 10^{-4} kmol/m^3 and with k_{AL}=4·10^{-5} m/s-the numerically predicted E_A=7.6 which is lower than the corresponding value of E_A=10.8 computed with k_{AL}=2.8·10^{-5} m/s. In contrast, the lowering of k_{AL} to 2·10^{-5} m/s results in an increase in the enhancement factor up to E=15.

The analysis of the influence of different CO_2 loadings on the enhancement factor predicted by the detailed mathematical model is shown in Fig. 5. In this case, it is not possible to compare the numerical solution with the approximate one as the latter is valid only for the case where the CO_2 bulk concentration is equal to 0. The computed results demonstrate that the enhancement factor predicted from the detailed model decreases with the increase of CO_2 loading. The lower curve (dashed line) was generated from the numerical model by neglecting the CO_2/OH$^-$ reaction. It can be observed that the contribution of reaction (2) is very small and it becomes insignificant as the CO_2 loading increases.

CONCLUSIONS

The CO_2 absorption rate into aqueous N-methyldiethanolamine solutions was studied experimentally in the temperature range of 293-333 K. A mathematical mass-transfer model based on the film theory was developed to interpret the experimental results. In this model, four chemical reactions that occur in the CO_2-H_2O-MDEA system are included and considered to be reversible. The initial absorption rates predicted by the use of the proposed model are consistent with the experimentally observed rates. The simulations of absorption rates, which were obtained from the detailed model after excluding the rate of CO_2/OH$^-$ reaction, show that the contribution of this reaction is negligible for high CO_2 partial pressures. Only at very low CO_2 partial pressure, the hydroxide contribution is significant. For higher CO_2 partial pressures which were applied in the present experiments, the OH$^-$ becomes depleted in the liquid film and its contribution to the total absorption rate is negligible. Hence, the numerical results of the proposed model were found to be in good agreement with analytical solution of mass transfer with chemical reaction for the case of a single, irreversible chemical reaction between CO_2 and MDEA taking place in the fast pseudo-first order regime over the whole range of operating conditions applied in the present work.

The applicability of the detailed mathematical model was demonstrated by performing simulations of mass transfer of CO_2 into aqueous MDEA solutions over a wide range of operating conditions, beyond the regime where the approximate solution is valid. The model results are in good agreement with the numerical solutions of previous authors despite different modeling approaches [15-18]. The influence of CO_2/OH$^-$ reaction on the CO_2 absorption rate for partially CO_2 loaded amine solution was demonstrated. To conclude, in the operating conditions encountered in practice which involve the loaded amine solution, the influence of this reaction on the predicted enhancement factor can be neglected.

ACKNOWLEDGEMENTS

This work was funded by the Ministry of Science and Higher Education of Poland (Project No. N N209 102937).

NOMENCLATURE

A : gas-liquid interfacial area [m^2]
C : concentration [kmol·m^{-3}]
D : diffusion coefficient [m^2·s^{-1}]
d_s : stirrer diameter [m]
E_A : enhancement factor
E_i : enhancement factor for an instantaneous reaction
H : Henry's law constant for CO_2 [Pa·m^3·mol^{-1}]
k_{iL} : liquid side mass transfer coefficient of species i [m·s^{-1}]
k_j : rate coefficient of reaction j [m^3·kmol^{-1}·s^{-1}]
K_j : equilibrium constant of reaction j (-), [m^3/kmol]
Ha : Hatta number
n : number of experimental data
n_s : stirring speed [s^{-1}]
N^*_{AL} : absorption rate of CO_2 at the interface [kmol·m^{-2}·s^{-1}]
p : partial pressure [Pa]
r_j : chemical reaction rate [kmol·m^{-3}·s^{-1}]
R : universal gas constant, 8.3143 [J/mol·K]
Re_L : Reynolds number, $Re_L = \frac{n_s d_s^2 \rho_L}{\eta_L}$
s : dimensionless distance

Sc_L : Schmidt number, $Sc_L = \frac{\eta_L}{\rho_L D_{AL}}$

Sh_L: Sherwood number, $Sh_L = \frac{k_{AL} d_s}{D_{AL}}$

t : time [s]

T : temperature [K]

V : volume [m^3]

Greek Letters

δ : refers to a liquid bulk

α : mole ratio in the liquid phase [mol CO_2/mol MDEA]

ρ : density [$kg \cdot m^{-3}$]

η : viscosity [Pa·s]

Φ : dimensionless concentration

ν_{ij} : the stoichiometric coefficient of species i in the reaction j

Subscripts

A : CO_2

B : MDEA

C : $MDEAH^+$

D : HCO_{3-}

E : OH^-

F : CO_3^{-2}

G : gas phase

L : liquid phase

i : component i

Supercripts

* : refers to a gas-liquid interface or equilibrium conditions

0 : refers to an initial state

ov : overall

REFERENCES

1. A. L. Kohl and R. B. Nielsen, Gas Purification (5th Ed.), Gulf Publishing Co., Houston (1997).
2. R. J. Notz, I. Tönnies, N. McCann, G. Scheffknecht and H. Hasse, *Chem. Eng. Technol.*, **34**(2), 163 (2011).
3. R. J. Notz, N. Asprion, I. Clause and H. Hasse, *Chem. Eng. Res. Des.*, **85**(4), 510 (2007).
4. N. Haimour, A. Bidarian and O. Sandall, *Chem. Eng. Sci.*, **42**, 1393 (1987).
5. R. J. Littel, W. P. M. Van Swaaij and G. F. Versteeg, *AIChE J.*, **36**(11), 1633 (1990).
6. R. A. Tomsej and F. D. Otto, *Chem. Eng. Sci.*, *AIChE J.*, **35**(5), 573 (1989).
7. F. Pani, A. Gaunand, R. Cadours, C. Bouallou and D. Richon, *J. Chem. Eng. Data*, **42**(2), 353 (1997).
8. J.-J. Ko and M.-H. Li, *Chem. Eng. Sci.*, **55**(9), 4139 (2000).
9. W. Moniuk and R. Pohorecki, *Inżynieria Chemiczna i Procesowa*, **21**(1), 183 (2000).
10. Jamal, A. Meisen, C. Jim Lim, *Chem. Eng. Sci.*, **61**, 6571 (2006).
11. Jamal, A. Meisen, C. Jim Lim, *Chem. Eng. Sci.*, **61**, 6590 (2006).
12. A. Benamor and M. K. Aroua, *J. Chem. Eng.*, **24**, 16 (2007).
13. P. D. Vaidya and E. Y. Kenig, *Chem. Eng. Technol.*, **30**(11), 1467 (2007).
14. T. L. Donaldson and Y. N. Nguyen, *Ind. Eng. Chem. Fundam.*, **19**, 260 (1980).
15. D. A. Glasscock and G. T. Rochelle, *AIChE J.*, **35**, 1271 (1989).
16. E. B. Rinker, S. S. Ashour and O. C. Sandall, *Chem. Eng. Sci.*, **50**, 755 (1995).
17. R. Cadours and C. Bouallou, *Ind. Eng. Chem. Res.*, **37**(3), 1063 (1998).
18. A. Kabouche, A. H. Meniai and M. Bencheikk-lehocine, *Chem. Eng. Technol.*, **28**(1), 67 (2005).
19. D. W. Marguardt, *J. Soc. Indust. Appl. Math.*, **11**, 431 **(**1963).
20. R. Zarzycki and A. Chacuk, *Absorption: Fundamentals and applications*, Pergamon Press, Oxford (1993).
21. H. Kierzkowska-Pawlak and A. Chacuk, *Chem. Eng. J.*, **168**(1), 367 (2011).
22. G. F. Versteeg and W. P. M. Van Swaaij, *J. Chem. Eng. Data*, **33**(1), 29 (1988).
23. H. A. Al-Ghawas, D. P. Hagewiesche, G. Ruiz-Ibanez and O. C. Sandall, *J. Chem. Eng. Data*, **34**(4), 385 **(**1989).
24. R. Cadours, H. Bouallou and A. Gaunand, *Ind. Eng. Chem. Res.*, **36**, 5384 (1997).
25. R. W. Pinsent, L. Pearson and F. J. W. Roughton, *Trans. Faraday Soc.*, **52**, 1512 (1956).